Journal of the Nigerian Mathematical Society
Vol. 36, pp. 163-190, 2017

EFFECTS OF EXOTHERMIC CHEMICAL REACTION WITH ARRHENIUS ACTIVATION ENERGY, NON-UNIFORM HEAT SOURCE/SINK ON MHD STAGNATION POINT FLOW OF A CASSON FLUID OVER A NONLINEAR STRETCHING SHEET WITH VARIABLE FLUID PROPERTIES AND SLIP CONDITIONS

M. MONICA [1], J. SUCHARITHA AND CH KISHORE

ABSTRACT. In this analysis, effects of exothermic chemical reactions with Arrhenius activation energy, non-uniform heat source/sink on magnetohydrodynamic stagnation point flow of a Casson fluid over a nonlinear stretching sheet with variable viscosity, thermal conductivity and slip boundary conditions have been investigated. An appropriate similarity transformations were used to transform the governing partial differential equations into coupled nonlinear ordinary differential equations. The transformed ordinary differential equations were then solved by efficient numerical technique known as Keller Box method. The various parameters such as Prandtl number (Pr), Eckert number (Ec), Magnetic parameter (M), Casson parameter (β), thermal radiation (R), non-uniform heat source/sink (A^*, B^*) , velocity ratio parameter(λ), nonlinear stretching parameter (n), chemical reaction rate constant (α), activation energy (E) , temperature dependent viscosity (ξ) , temperature dependent thermal conductivity (ϵ) and slip parameters (S_1, S_2, S_3) determining the velocity, temperature and concentration distributions, the local Skin friction coefficient, the local Nusselt number and the local Sherwood number governing such a flow were also analyzed. On analysis it has been found that the Skin friction coefficient, Local Nusselt number and Local Sherwood number decreases with respect to velocity, thermal and concentration slips respectively.

Keywords and phrases: Exothermic reactions , thermal radiation , non-uniform heat source/sink , Nonlinear stretching sheet , slip boundary conditions , variable viscosity and thermal conductivity
2010 Mathematical Subject Classification: A80

Received by the editors January 16, 2016; Revised: June 29, 2016; Accepted: July 09, 2016
www.nigerianmathematicalsociety.org
[1]Corresponding author

1. INTRODUCTION

The study of stagnation point flow has attracted many scientists and investigators and has been a subject of great interest for the last several decades due to its importance in industrial and scientific applications. Some of the applications are cooling of electronic devices by fans, cooling of nuclear reactors during emergency shutdown, solar central receivers exposed to wind currents, and many hydrodynamic processes in engineering applications. Stagnation-point flow, describing the fluid motion near the stagnation region of a circular body, exists for both the cases of a fixed or moving body in a fluid. Hiemenz [1] first initiated the two-dimensional stagnation flow towards a stationary semi-infinite wall by using a similarity transformation, to reduce the Navier-Stokes equations to a nonlinear ordinary differential equation. Homann [2] then extended this problem to the case of axisymmetric stagnation-point flow. Stagnation point flows have been studied by Pai [3], Schlichting [4] and Bansal [5] etc., .

The work on the stagnation-point flow has been carried out still by many investigators in various ways. Accordingly, Chiam [6] studied the stagnation-point flow towards a stretching sheet and found no boundary layer structure near the sheet. Mahapatra and Gupta [7] discussed the same stagnation-point flow towards a stretching sheet and found two kinds of boundary layer near the sheet. They analyzed that a boundary layer is formed when the free stream velocity exceeds stretching velocity and an inverted boundary layer is formed when the free stream velocity is less than stretching velocity. By considering a special case of stretching sheet, the stagnation point flow on a two dimensional shrinking sheet and axisymmetric stagnation point flow on an axisymmetric shrinking sheet has been analyzed by Wang [8]. In contrast, Lok et al. [9] numerically studied non orthogonal stagnation point flow towards a stretching sheet. In his work, he determined that the obliqueness of a free stream line causes the shifting of the stagnation point towards the incoming flow. The stagnation-point flow over stretching sheet was further investigated by Nazar et al. [10], Layek et al. [11] where they explored some important properties.

The problem of non-linear stretching sheet for different cases of fluid flow has also been analyzed by different researchers. In view of this, Vajravelu [12] analyzed flow and heat transfer over a nonlinear stretching sheet. Cortell [13] extended the model proposed by [12] considering two different types of thermal boundary conditions

on the sheet, constant surface temperature and prescribed surface temperature. Prasad et al. [14] investigated the mixed convection heat transfer over a non-linear stretching surface with variable fluid properties. Hayat et al. [15] investigated MHD flow of a micropolar fluid near a stagnation-point towards a non-linear stretching surface. A.Raptis et al. [16] analyzed viscous flow over a non-linearly stretching sheet in the presence of a chemical reaction and magnetic field. Solutions for micropolar transport phenomena over a nonlinear stretching sheet has been investigated by R.Bhargava et al. [17].

During the past several years, it has been observed that a number of industrial fluids such as molten plastics, polymeric liquids, chemicals, cosmetics, pharmaceuticals, blood and food stuff exhibit non-Newtonian fluid behaviour. Different types of non-Newtonian fluids are viscoelastic fluid, couple stress fluid, second grade, micro polar fluid, power-law fluid, Casson fluid etc.,. The most important non-Newtonian fluid possessing a yield value is the Casson fluid which has significant applications in polymer processing industries and biomechanics. Casson fluid is defined as a shear thinning fluid which is assumed to have an infinite viscosity at zero rate of shear. Cassons constitutive equations are found to describe accurately the low curves of suspensions of pigments in lithographic varnishes used for preparation of printing inks and silicon suspensions [18]. The unsteady boundary layer flow and heat transfer of a Casson fluid over a moving flat plate with a parallel free stream was studied by Mustafa et al. [19]. Later on, several researchers studied Casson fluid for different flow situations and configurations [20]-[26].

Fluids exhibiting slip are important in technological applications such as in the polishing of artificial heart valves and internal cavities. With a slip at the wall boundary, the flow behaviour and the shear stress in the fluid are quite different from those in the no-slip flows. The effects of partial slip on the boundary layer stagnation-point flow and heat transfer towards a shrinking surface has been investigated by Bhattacharyya et al. [27]. The slip effect on MHD boundary layer flow over a flat plate was also analyzed by Bhattacharyya et al. [28]. Fang et al. [29] obtained the exact analytic solution of MHD flow under slip condition over a permeable stretching sheet. Studies concerned to slip flows under different flow configurations were obtained from literature [30]-[35].

An exothermic reaction is a chemical or physical reaction that releases heat. It gives net energy to its surroundings. That is, the

energy needed to initiate the reaction is less than the energy that is subsequently released. Energy is obtained from chemical bonds. Energy is required to break these bonds and it is released to form bonds. There is specific bond energy depending upon each type of bond. It can be predicted whether a chemical reaction will release or require heat by using bond energies. When there is more energy used for either the bonds to be formed or to break the bonds, heat is given out. This is known as an exothermic reaction. When a reaction requires an input of energy, it is known as an endothermic reaction. The ability to break bonds is activation energy. In boundary layer flows one important criteria that is generally not encountered is the species chemical reactions with finite Arrhenius activation energy. The Arrhenius law is usually of the form (Tencer et al. [36]).

$$K = B(T - T_\infty)^w exp\left[\frac{-E_a}{k(T - T_\infty)}\right] \tag{1}$$

where K is the rate constant of chemical reaction and B is the pre exponential factor simply pre factor (constant) is based on the fact that increasing the temperature frequently causes a marked increase in the rate of reactions. E_a is the activation energy, and $k = 8.61 \times 10^{-5} eV/K$ is the Boltzmann constant which is the physical constant relating energy at the individual particle level with temperature observed at the collective or bulk level. Bestman [37] and Alabraba et al. [38] took into account the effect of the Arrhenius activation energy under the different physical conditions. Recently Kandasamy et al. [39] studied the combined effects of chemical reaction, heat and mass transfer along a wedge with heat source and concentration in the presence of suction or injection. Recently Makinde et al. [40], [41] studied the problems of unsteady convection with chemical reaction and radiative heat transfer past a flat porous plate moving through a binary mixture in an optically thin environment. More recently Abdul Maleque [42], [43] investigated the similarity solution on unsteady incompressible fluid flow with binary chemical reactions and activation energy. It is well known that physical properties like viscosity and thermal conductivity depend upon temperature. In many systems, the rise in temperature affects the viscosity of the fluid and so the fluid viscosity can no longer be assumed constant. In order to predict the flow behavior accurately, it is necessary to take into account the viscosity variation with temperature. The increase of temperature leads to a

local increase in the transport phenomena by reducing the viscosity across the momentum boundary layer and so the heat transfer rate at the wall is also affected greatly. In industrial systems, fluids can be subjected to extreme conditions such as high temperature, pressure, high shear rates and external heating (Ambient Temperature) and each of these factors can lead to high temperature being generated within the fluid. Heat transfer in MHD fluid flow over a stretching sheet with variable thermal conductivity, non-uniform heat source and radiation was investigated by Abel [44]. Recently, Animasaun [45] presented the effects of some thermo-physical parameters on non-darcian MHD dissipative Casson fluid flow along linearly stretching vertical surface . Makinde [46] analyzed the effect of variable viscosity on thermal boundary layer over a permeable flat plate with radiation and a convective surface boundary condition. Salem and Fathy [47] investigated the effects of variable properties on MHD heat and mass transfer flow near a stagnation point towards a stretching sheet in a porous medium with thermal radiation and adopted the model of Prasad et al. [48].

Since no attempt has been made to analyze effects of exothermic chemical reactions with Arrhenius activation energy, non-uniform heat source/sink on magnetohydrodynamic stagnation point flow of a Casson fluid over a nonlinear stretching sheet with variable viscosity, thermal conductivity and slip boundary conditions so it is considered in this article. Using appropriate similarity tranformations, the governing partial differential equations were transformed into coupled non linear ordinary differential equations. The transformed ODE's were then solved by Keller Box method.

2. MATHEMATICAL FORMULATION

Consider the steady, two - dimensional flow of a viscous incompressible Casson fluid near a stagnation point over a stretching sheet coinciding with the plane $y = 0$ with surface temperature T_w and concentration C_w . The fluid occupies the upper half plane $y > 0$. The sheet is stretched horizontally by applying two equal and opposite forces along x-axis keeping the origin fixed. The stretching velocity of the sheet is $U_w(x) = cx^n$ where the x-component of the velocity varies non-linearly along it, $c > 0$ is constant of proportionality and n is a power index. The flow is subjected to the combined effect of thermal radiation and a transverse magnetic field of strength B_0 which is applied normal to the surface. The induced magnetic field is also assumed to be small compared to the

applied magnetic field; so it is neglected. It is also assumed that the ambient fluid is moved with a velocity $U_\infty(x) = ax^n$, where $a > 0$ is a constant. The ambient temperature and concentration, respectively are T_∞ and C_∞

The rheological equation of state for an isotropic and incompressible flow of the Casson fluid is given by

$$\tau_{ij} = 2(\mu_B + p_y/\sqrt{2\pi})e_{ij}, \quad \pi > \pi_c$$
$$2(\mu_B + p_y/\sqrt{2\pi_c})e_{ij}, \quad \pi < \pi_c$$

where μ_B and p_y are the plastic dynamic viscosity, yield stress of the fluid respectively. Similarly π is the product of the component of deformation rate with itself, $\pi = e_{ij}e_{ij}$, e_{ij} is the (i, j)-th component of the deformation rate and π_c is a critical value of this product based on the non-Newtonian model.

p_y is the yield stress of the fluid, mathematically expressed as

$$p_y = \frac{\mu_B\sqrt{2\pi}}{\beta}$$

$$\mu = \mu_B + \left(\frac{p_y}{\sqrt{2\pi}}\right)$$

The kinematics viscosity of Casson fluid is now depending on plastic dynamic viscosity μ_B , density ρ and Casson parameter β.

$$\nu = \frac{\mu_B}{\rho}(1 + \frac{1}{\beta})$$

In this theoretical study, it is assumed that the plastic dynamic viscosity of the non-Newtonian fluid together with its thermal conductivity varies as a linear function of temperature, (See Batchelor [49]). Following Prasad et al. [48]

$$\mu_B(T) = \mu_B^*[a + b(T_w - T)] \; and \; \kappa(T) = \kappa^*[a + \gamma(T - T_\infty)]$$

where μ^* is the constant value of the coefficient of viscosity far from the sheet, κ^* is the constant value of the coefficient of thermal conductivity far from the sheet, a, b and γ are constant; the case when a = 1 is considered only.

Under the above assumptions, the governing equations are

$$\frac{\partial u}{\partial x} + \frac{\partial v}{\partial y} = 0 \tag{2}$$

$$u\frac{\partial u}{\partial x} + v\frac{\partial u}{\partial y} = U_\infty\frac{\partial U_\infty}{\partial x} + \frac{\mu_B(T)}{\rho}(1 + \frac{1}{\beta})\frac{\partial^2 u}{\partial y^2}$$

$$+\frac{1}{\rho}(1+\frac{1}{\beta})\frac{\partial u}{\partial y}\frac{\partial T}{\partial y}\frac{\partial \mu_B(T)}{\partial T} - \frac{\sigma B^2(x)}{\rho}(u-U_\infty) \tag{3}$$

$$\begin{aligned} u\tfrac{\partial T}{\partial x} + v\tfrac{\partial T}{\partial y} &= \frac{\kappa(T)}{\rho C_p}\frac{\partial^2 T}{\partial y^2} + (1+\frac{1}{\beta})\frac{\mu_B(T)}{\rho C_p}(\frac{\partial u}{\partial y})^2 \\ &+\tfrac{1}{\rho C_p}(\tfrac{\partial T}{\partial y})^2\tfrac{\partial \kappa(T)}{\partial T} - \tfrac{1}{\rho C_p}\tfrac{\partial q_r}{\partial y} + \tfrac{q'''}{\rho C_p} \\ &+\tfrac{k_r^2}{\rho C_p}(T-T_\infty)^w exp\left[\tfrac{-E_a}{k(T-T_\infty)}\right](C-C_\infty) \end{aligned} \tag{4}$$

$$u\frac{\partial C}{\partial x} + v\frac{\partial C}{\partial y} = D\frac{\partial^2 C}{\partial y^2} - k_r^2(T-T_\infty)^w exp\left[\frac{-E_a}{k(T-T_\infty)}\right](C-C_\infty) \tag{5}$$

where x and y denotes the cartesian coordinates along and normal to the sheet respectively, u, v are the velocity components in x, y direction respectively, ν is the kinematic viscosity, ρ is the viscosity, $\beta = \mu_B\sqrt{2\pi_c}/p_y$ is the Casson fluid parameter, κ is the thermal diffusivity of the fluid, C_p is the specific heat, $B = B_0 x^{(n-1)/2}$ is the magnetic field, k_r^2 is the exothermic chemical reaction rate constant, $(T-T_\infty)^w exp\left[\frac{-E_a}{k(T-T_\infty)}\right]$ is the Arrhenius function, where w is a unit less constant exponent fitted rate constants typically lie in the range $-1 < w < 1$.

q''' is the non-uniform heat source which is modelled as

$$q''' = \frac{\kappa U_w(x)}{x\nu}[A^*(T_w - T_\infty)f' + B^*(T-T_\infty)] \tag{6}$$

where A^* and B^* are parameters of the space and temperature dependent internal heat generation/absorption. The case $A^* > 0$ and $B^* > 0$ corresponds to internal heat generation while $A^* < 0$ and $B^* < 0$ corresponds to the internal heat absorption.

Following Rosseland approximation, the radiative heat flux q_r is modelled as

$$q_r = -\frac{4\sigma^*}{3k^*}\frac{\partial T^4}{\partial y} \tag{7}$$

where σ^* is the Stefan-Boltzmann constant and k^* is the absorption coefficient. Assuming that the differences in temperature within the flow are such that T^4 can be expressed as a linear combination of the temperature, we expand T^4 in a Taylors series about T_∞ as follows

$$T^4 = T_\infty^4 + 4T_\infty^3(T-T_\infty) + 6T_\infty^2(T-T_\infty)^2 + ...$$

and neglecting the higher order terms beyond first degree in $(T - T_\infty)$ we get

$$T^4 \cong -3T_\infty^4 + 4T_\infty^3 T \tag{8}$$

substituting eq.(8) in eq.(7) we get

$$\frac{\partial q_r}{\partial y} = -\frac{16T_\infty^3\sigma^*}{3k^*}\frac{\partial^2 T}{\partial y^2} \tag{9}$$

The suitable boundary conditions for (2) - (5) are given by

$$u = U_w(x) + L(1+\tfrac{1}{\beta})\tfrac{\partial u}{\partial y},\ v = 0,\ T = T_w + K_1\tfrac{\partial T}{\partial y},$$
$$C = C_w + K_2\tfrac{\partial C}{\partial y} \text{ at } y = 0$$
$$u \to U_\infty,\ T \to T_\infty,\ C \to C_\infty \text{ as } y \to \infty$$

With the help of following similarity transformations

$$u = cx^n f'(\eta),\ v = -\sqrt{\tfrac{c\nu(n+1)}{2}}x^{(n-1)/2}[f(\eta) + \tfrac{n-1}{n+1}\eta f'(\eta)]$$
$$\theta(\eta) = \tfrac{T-T_\infty}{T_w-T_\infty},\ \phi(\eta) = \tfrac{C-C_\infty}{C_w-C_\infty},\ \eta = y\sqrt{\tfrac{c(n+1)}{2\nu}}x^{(n-1)/2}$$

The equations (3), (4) and (5) are transformed into coupled non-linear ordinary differential equations as follows.

$$\begin{gathered}(1+\tfrac{1}{\beta})(1+\xi-\theta\xi)f''' - \xi(1+\tfrac{1}{\beta})f''\theta' + ff'' \\ -\tfrac{2n}{n+1}(f'^2 - \lambda^2) + M(\lambda - f') = 0\end{gathered} \tag{10}$$

$$\begin{gathered}(1+\epsilon\theta+\tfrac{4R}{3})\theta'' + \epsilon\theta'^2 + Prf\theta' + (1+\xi-\theta\xi)(1+\tfrac{1}{\beta})Pr.Ec.f''^2 \\ +\tfrac{2}{n+1}(A^*f' + B^*\theta) + \alpha^2 Pr.exp\left(\tfrac{-E}{\theta}\right)\theta^w\phi = 0\end{gathered} \tag{11}$$

$$\phi'' + Scf\phi' - Sc.\alpha^2.exp\left(\frac{-E}{\theta}\right)\theta^w\phi = 0 \tag{12}$$

and the boundary conditions are transformed into

$$\begin{gathered}f'(\eta) = 1 + S_1(1+\tfrac{1}{\beta})f''(0),\ f(\eta) = 0, \\ \theta(\eta) = 1 + S_2\theta'(0),\ \phi(\eta) = 1 + S_3\phi'(0)\ at\ \eta = 0 \\ f'(\eta) \to \lambda,\ \theta(\eta) \to 0,\ \phi(\eta) \to 0\ as\ \eta \to \infty\end{gathered} \tag{13}$$

where prime denotes the differentiation with respect to η and $Pr = \frac{\mu C_p}{\kappa}$ is the Prandtl Number, $M = \frac{2\sigma B_0^2}{\rho c(n+1)}$ is the magnetic parameter, $R = \frac{4\sigma^* T_\infty^3}{kk^*}$ is the radiation parameter, $Sc = \frac{\gamma}{D}$ is the Schmidt number, $\xi = b(T_w - T_\infty)$ is the temperature dependent viscosity parameter , $\epsilon = \gamma(T_w - T_\infty)$ is the temperature dependent thermal conductivity parameter ;the non dimensional activation energy $E = \frac{E_a}{k(T-T_\infty)}$, the dimensionless chemical reaction rate constant $\alpha^2 = \frac{2k_r^2(T-T_\infty)^w}{c(n+1)x^{(n-1)}}$, $Ec = \frac{U_w^2}{C_p(T_w-T_\infty)}$ is the Eckert number and $\lambda = \frac{a}{c}$ is the velocity ratio parameter, $S_1 = Lx^{(n-1)/2}\sqrt{\frac{c(n+1)}{2\nu}}$, $S_2 = K_1x^{(n-1)/2}\sqrt{\frac{c(n+1)}{2\nu}}$, $S_3 = K_2x^{(n-1)/2}\sqrt{\frac{c(n+1)}{2\nu}}$ are the velocity,

thermal and concentration slips respectively.
The quantities of practical interest are the Skin friction coefficient C_f , the Local Nusselt number Nu_x and the Local Sherwood number Sh_x which are defined as

$$C_f = \frac{\tau_w}{\rho U_w^2},\ Nu_x = \frac{x q_w}{k(T_w - T_\infty)},\ Sh_x = \frac{x m_w}{D(C_w - C_\infty)}$$

where τ_w is the shear stress or skin friction along the stretching sheet q_w is the heat flux from the sheet and m_w is the mass flux from the sheet.

$$\tau_w = \mu \left\{\frac{\partial u}{\partial y}\right\}_{y=0},\ q_w = -\left(k + \frac{16\sigma^* T_\infty^3}{3k^*}\right)\left\{\frac{\partial T}{\partial y}\right\}_{y=0},$$
$$m_w = -D\left\{\frac{\partial C}{\partial y}\right\}_{y=0}$$

Hence the dimensionless form of Skin friction C_f , the Local Nusselt number Nu_x and the Local Sherwood number Sh_x are given by

$$C_f = Re_x^{-1/2}(1 + \frac{1}{\beta})\sqrt{\frac{(n+1)}{2}}\left\{f''(0)\right\},$$
$$Nu_x = Re_x^{1/2}\sqrt{\frac{(n+1)}{2}}(1 + \frac{4R}{3})\left\{-\theta'(0)\right\},$$
$$Sh_x = Re_x^{1/2}\sqrt{\frac{(n+1)}{2}}\left\{-\phi'(0)\right\}$$

where $Re_x = U_w x/\nu$ is the local Reynolds number.

3. NUMERICAL DISCUSSION

The numerical solutions are obtained for velocity, temperature and concentration profiles for various values of governing parameters by adopting numerical scheme known as Keller Box method. Effect of magnetic parameter, velocity ratio parameter, nonlinear stretching parameter, Prandtl number, radiation parameter, Eckert number, chemical reaction parameter, non-uniform heat source /sink, variable viscosity, thermal conductivity, activation energy on velocity and temperature profiles has been clearly analyzed including with its physical quantities of significance. The values of the parameters are fixed as $\beta = 10$, $\lambda = 0.2$, Pr = 0.71, n = 2, M = 2, Ec = 0.05, R = 1, Sc = 0.7, E = 1, $\alpha = 1.2$, $\xi = 0.2$, $\epsilon = 0.1$, $S_1 = S_2 = S_3 = 0.1, A^* = B^* = 0.01$ unless otherwise specified.

Fig 2 depicts the effect of the velocity ratio parameter on the flow field velocity. It can be observed that for $\lambda < 1$ i.e., when the stretching velocity of the sheet exceeds the free stream velocity, the velocity of the fluid and the boundary layer thickness increases with an increase in λ. Moreover, for $\lambda > 1$ i.e., when the free stream exceeds the stretching velocity, the flow velocity increases and the boundary layer thickness decreases with an increase in λ. If $\lambda = 1$ i.e., when the stretching and free stream velocities are equal, then there is no boundary layer of Casson fluid flow near the sheet.

Figure 3 indicates the velocity profile for various values of nonlinear stretching parameter n. It is depicted that the velocity of the fluid decreases with an increase in power index n. Figure 4 indicates the effect of magnetic parameter M on velocity profile. The velocity of the fluid decreases with an increase in M. This causes retarding effect on the flow field leading to the prominent reduction in velocity due to Lorentz force effect. Therefore, the Lorentz force increases the opposition of the flow of fluid reducing the velocity of the flow.

Fig 5 and Fig 6 indicates the effect of Casson parameter β on velocity and temperature profiles respectively. It can be noticed from Fig 5 that the velocity of the fluid decreases when β increases. Actually an increase in Casson parameter β offers more resistance in the fluid flow. An increase in β implies a decrease in yield stress p_y of the Casson fluid and increase in the value of plastic dynamic viscosity μ_B; this causes resistance in the flow of fluid. In the vicinity of the sheet the velocity profile curves for larger values of β are little higher than for those with smaller values of β. However, as we move just far from the sheet within the velocity boundary layer, the yield stress p_y increases implies the plastic dynamic viscosity μ_B decreases, the curves for smaller values of β tend to override for larger values of β. Fig 6 shows that an increase in β causes the temperature to decrease which implies that the thermal boundary layer decreases.

The influence of Eckert number Ec is depicted in Fig 7. It illustrates that the temperature increases with an increase in Ec. The viscous dissipation produces heat due to drag between the fluid particles and this extra heat causes an increase of the initial fluid temperature.

The effect of radiation parameter is depicted in Fig 8. It shows that temperature increases with an increase in R. This is because; increase in radiation parameter provides more heat to fluid that

causes an enhancement in the temperature and thermal boundary layer thickness.

Fig 9 shows the temperature profile for various values of Pr. It is clear that the dimensionless parameter θ decreases with the increase in Prandtl number. Since the Prandtl number is the ratio of momentum diffusivity to thermal diffusivity; it reduces the thermal boundary layer thickness. In general the Prandtl number is used in heat transfer problems to reduce the relative thickening of the momentum and the thermal boundary layers.

Fig 10 depicts the variation of velocity with respect to velocity slip parameter S_1. The velocity graph decreases as the values of S_1increases. Hence the momentum boundary layer thickness decreases. The effect of thermal velocity parameter S_2 on temperature profile is displayed in Fig 11. It reveals that the thermal boundary layer thickness decreases when the values of S_2 increases. Fig 12 indicates the effect of concentration slip parameter S_3 on concentration profile. It can be observed that the concentration boundary layer thickness decreases with an increase in S_3.

Figures 13 and 14 indicates the effects of the heat source/sink parameter on the temperature. The heat generation/absorption clearly affects the flow and temperature of the fluid. It is the cumulative influence of the flow and temperature-dependent heat source/sink parameter that determines the extent to which temperature falls or rises in the boundary layer region. From the graphs it is clear that, the thermal boundary layer generates energy for increasing values of $A^* > 0, B^* > 0$ and this causes the magnitude of temperature to increase, where as for decreasing values of $A^* < 0, B^* < 0$ energy is absorbed thus resulting the temperature to drop significantly near the boundary layer. Non-uniform heat sinks corresponding to $A^* < 0, B^* < 0$ can contribute to quenching the heat from stretching sheet effectively.

Figures 15 and 16 shows the effects of chemical reaction rate constant α on temperature and concentration profiles when the magnitude of thermal radiation is high (i.e., R = 1) and in the presence of non-uniform heat source/sink (i.e.$A^* = B^* = 0.01$). We observe that chemical reaction rate constant α^2 is always positive. The graph clearly indicates that as the chemical reaction rate constant α increases, the temperature decreases since the number of molecules that carry enough energy to react when they collide also decreases. Therefore the thermal boundary layer thickness

decreases. The concentration profile increases with the increasing values of α.

Effects of activation energy (E) on the temperature and the concentration profiles are shown in Figures 17 and 18, respectively. Equation (1) suggests that the activation energy is dependent on temperature. From Fig 17 we observe that when activation energy increases the temperature profile decreases due to the presence of thermal radiation. From Equation (1), we observe that chemical reaction rate (K) decreases with the increasing values of activation energy E_a. We also observe from Equation (17) that increase in activation energy (E) leads to decrease $\alpha^2.exp\left(\frac{-E}{\theta}\right)$ as well as to increase the concentration profiles shown in Figure 18.

Fig. 19 depicts the variation of velocity profiles for different values of temperature dependent plastic dynamic viscosity parameter ξ. It is observed that when Casson fluid is treated as fluid with constant plastic dynamic viscosity throughout the boundary layer, the velocity is found to be very small in quantity throughout the boundary layer compared to when treated as variable plastic dynamic viscosity. It shows that with increasing ξ the transport phenomena across the momentum boundary layer increases. Actually ξ increases implies the resulting temperature at constant value of b i.e., $b(T_w - T_\infty)$ increases which makes the bond between Casson fluids to become weaker and the strength of plastic dynamic viscosity decreases effectively.

Figure 20 represents the effect of temperature dependent plastic dynamic viscosity parameter ξ on temperature profiles. It can be observed that the temperature decreases with the increase in the magnitude of temperature dependent plastic dynamic viscosity parameter. Decrease in temperature profiles across the thermal boundary layer means a decrease in the velocity of the Casson fluid. In this case, the fluid particles undergo two opposite forces which are: (i) one force increases the velocity of the fluid due to decrease in the fluid viscosity with increasing ξ , (ii) the second force decreases the velocity of the fluid due to decrease in temperature; since temperature profile decreases with increasing ξ . Very near the vertical surface, as the temperature profile is high, the first force dominates and far away from the surface, the temperature profile is low; this implies that the second force dominates in that region.

Fig 21 reveals the influence of temperature dependent variable thermal conductivity over temperature profile. It is observed that

as the temperature dependent variable thermal conductivity increases, the temperature increases significantly.

Finally, a comparison with previously published papers has been done in order to check the accuracy of the present results. Tables 1 and 2 represents the numerical values of the skin friction coefficient $f''(0)$ and local Nusselt number $-\theta'(0)$ for different values of A, Ec, n and Pr are in excellent agreement with the result published in Andersson [31], Hayat et al.[35] and Cortell[13].

Table 3 shows the variations of skin friction coefficient $-(1 + \frac{1}{\beta})f''(0)$ for various values of M, λ, β, ξ and A. It can be observed from the table that the values of skin friction coefficient increases when magnetic field and temperature dependent plastic dynamic viscosity increases whereas it decreases for remaining parameters. Table 4 presents the variation in Local Nusselt number with respect to various flow parameters. It reveals that temperature gradient $-\theta'(0)$ decreases for all the parameters but for the Prandtl number, casson parameter and chemical reaction rate constant $-\theta'(0)$ increases. Table 5 shows the comparison of Local Sherwood number $-\phi'(0)$ in relation to chemical reaction parameter, activation energy, Schmidt number and Concentration slip parameter. $-\phi'(0)$ increases for Schmidt parameter whereas for other parameters it decreases.

4. CONCLUDING REMARKS

In the present study,effects of exothermic chemical reactions with Arrhenius activation energy, thermal radiation, non-uniform heat source/sink on magnetohydrodynamic stagnation point flow of a Casson fluid over a nonlinear stretching sheet with variable viscosity, thermal conductivity and slip boundary conditions are investigated. The numerical solution is obtained by Keller Box Method. The effects of various governing parameters on heat flow characteristics were analyzed. Briefly the above discussion can be summarized as follows.

- The velocity of the fluid decreases with an increase in nonlinear stretching parameter.
- The velocity boundary layer thickness reduces for magnetic parameter M.
- An increase in the variable plastic dynamic viscosity parameter of Casson fluid corresponds to an increase in the velocity profiles and a decrease in temperature throughout the boundary layer.

- Both the Eckert number and the radiation parameter increases the thermal boundary layer thickness where as the Prandtl number decreases it.
- An increase in chemical reaction parameter decreases the concentration boundary layer thickness.
- The velocity slip parameter S_1 reduces the thickness of the momentum boundary layer.
- The thickness of thermal boundary layer decreases with an increase in thermal slip parameter.
- The concentration boundary layer thickness decreases with an increase in solutal slip parameter.
- The effect of temperature dependent heat source/sink parameters is to generate temperature for increasing positive values and absorb temperature for decreasing negative values.
- Temperature dependent plastic dynamic viscosity and thermal conductivity increases velocity profiles significantly whereas the temperature dependent plastic dynamic viscosity decreases the temperature.
- Increase in the activation energy and chemical reaction rate constant decreases the temperature profile and increases the concentration profiles.

ACKNOWLEDGEMENTS

The author would like to thank the anonymous referee whose comments improved the original version of this manuscript and also UGC,BSR-RFSMS funding agency.

TABLE 1. Comparison of Skin friction coefficient $f''(0)$ for different values of S_1

S_1	Anderson[31]	Hayat[35]	Present result
0	1	1	1
0.1	0.8721	0.872	0.87208
0.2	0.7764	0.77637	0.77638
0.5	0.5912	0.591195	0.5912
2	0.284	0.283981	0.28398
5	0.1448	0.144841	0.14484
10	0.0812	0.081244	0.08124
20	0.0438	0.043782	0.04379
50	0.0186	0.018634	0.0186

TABLE 2. Comparison of Nusselt number $-\theta'(0)$ for different values of Ec, n

Ec	n	Cortell[13] Pr = 1	Present result	Cortell[13] Pr = 5	Present result
0	0.2	0.610262	0.6102	1.607175	1.60779
	0.5	0.595277	0.5952	1.586744	1.58678
	1.5	0.574537	0.57473	1.557463	1.5577
	3	0.564472	0.56466	1.542337	1.54318
	10	0.55496	0.55488	1.528573	1.52893
0.1	0.2	0.574985	0.57527	1.474764	1.47504
	0.5	0.556623	0.55678	1.436789	1.43703
	1.5	0.530966	0.53096	1.381861	1.38209
	3	0.517977	0.51803	1.352768	1.35376
	10	0.505121	0.50533	1.324772	1.3254

TABLE 3. Computed values of skin friction coefficient $-(1+\frac{1}{\beta})f''(0)$ for various values of M , λ , β , ξ and S_1

M	λ	β	S_1	ξ	$-(1+\frac{1}{\beta})f''(0)$
0					0.92009
1					1.14039
2					1.31147
	0.5				0.87967
	1				0
	1.5				-1.04641
		0.5			1.9482
		1.0			1.66845
		1.5			1.55261
			0.1		1.31147
			0.5		0.77338
			1		0.51671
				1.5	1.34761
				2.5	1.37063
				3.5	1.39043

TABLE 4. Computed values of Local Nusselt number $-\theta'(0)$ for various parameters

β	Pr	R	Ec	A^*	B^*	S_2	ϵ	ξ	α	E	$-\theta'(0)$
0.5											0.36733
1											0.3694
2											0.37131
	1										0.46177
	2										0.68968
	3										0.861
		0.5									0.45218
		1.5									0.32145
		2									0.28334
			0.5								0.31717
			1.5								0.19081
			2								0.12718
				- 0.04							0.39351
				0.01							0.37366
				0.04							0.36169
					- 0.04						0.39231
					0.01						0.37366
					0.04						0.36176
						0.1					0.37366
						0.5					0.35337
						1.5					0.28032
							1.5				0.26454
							2.5				0.22085
							3.5				0.19006
								1.5			0.37141
								2.5			0.36998
								3.5			0.36876
									0.5		0.24514
									1		0.31368
									1.5		0.50088
										0	0.01789
										1	0.37366
										1.5	0.62796

TABLE 5. Computed values of Local Sherwood number $-\phi^{'}(0)$ for various values of α, E, Sc and S_3

Sc	α	E	S_3	$-\phi^{'}(0)$
0.6				0.38131
0.7				0.23994
0.75				0.15074
	0.5			0.10144
	1			0.11578
	1.5			0.124
		0		0.95691
		1		0.11578
		1.5		0.43231
			0	0.11729
			0.5	0.11016
			1	0.10396

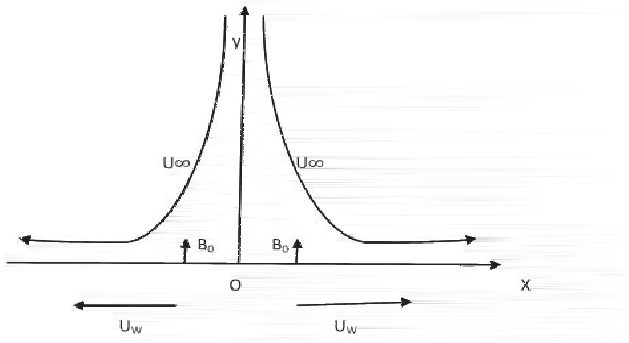

Fig. 1: Physical sketch

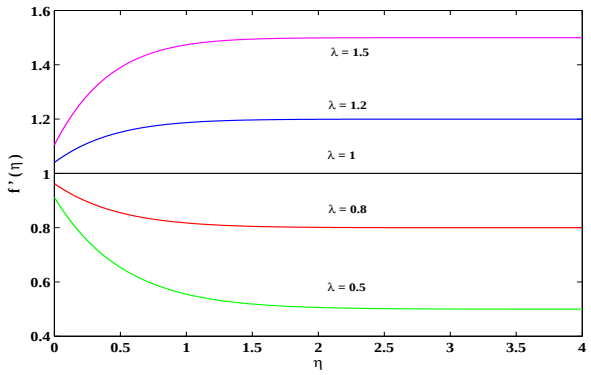

Fig. 2: Velocity profile for various values of velocity ratio parameter λ

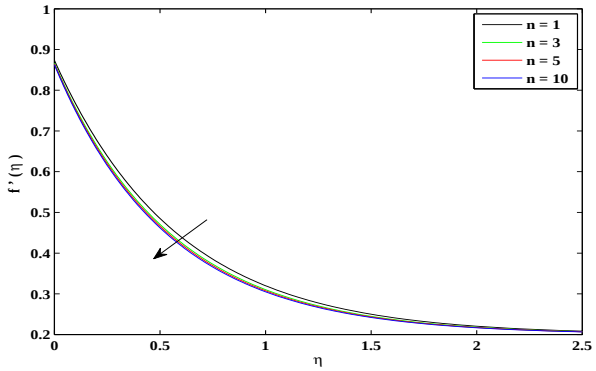

Fig. 3: Velocity profile for various values of nonlinear stretching parameter

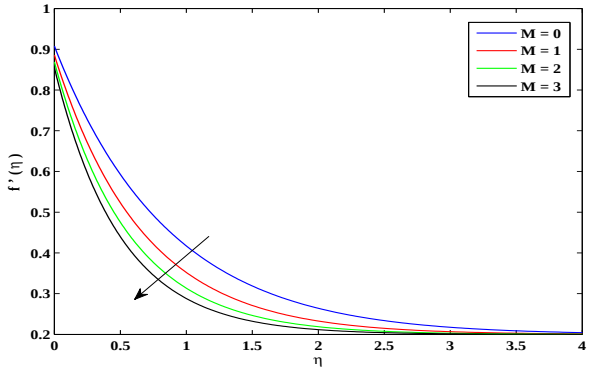

Fig. 4: Velocity profile for various values of M

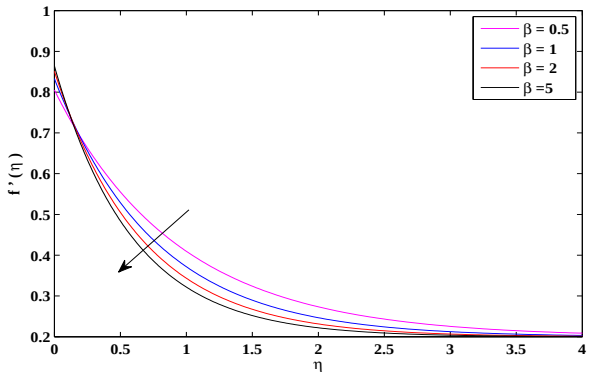

Fig. 5: Velocity profile for various values of β

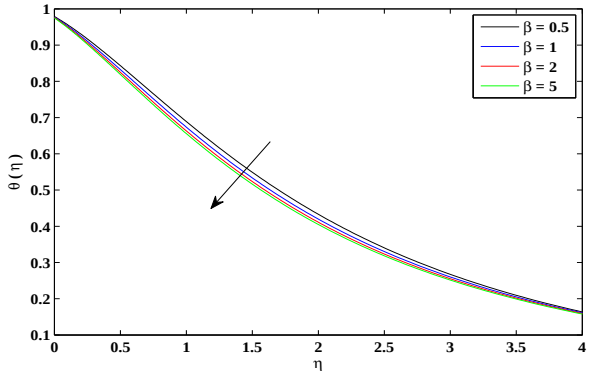

Fig. 6: Temperature profile for various values of β

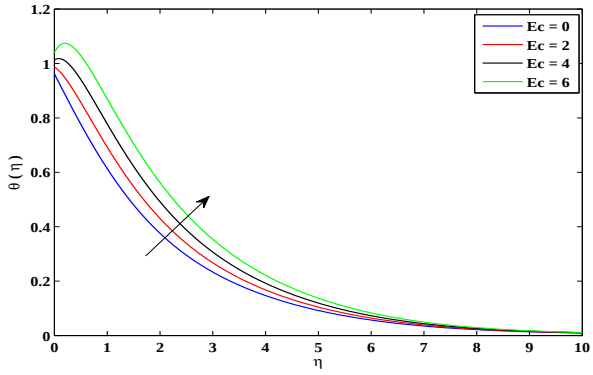

Fig. 7: Temperature profile for various values of Ec

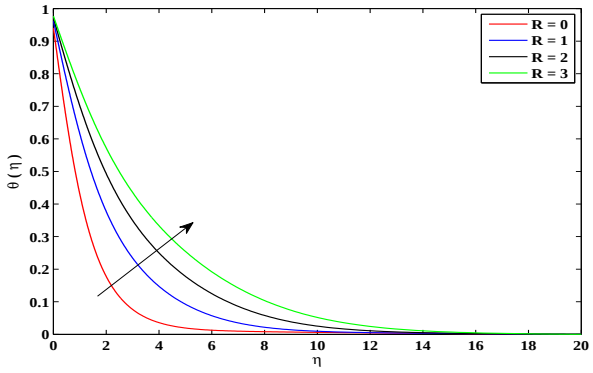

Fig. 8: Temperature profile for various values of R

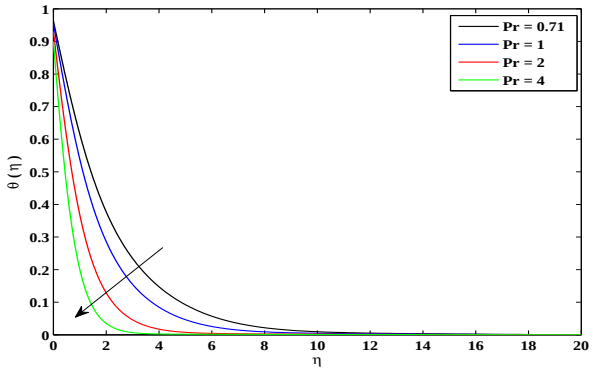

Fig. 9: Temperature profile for various values of Pr

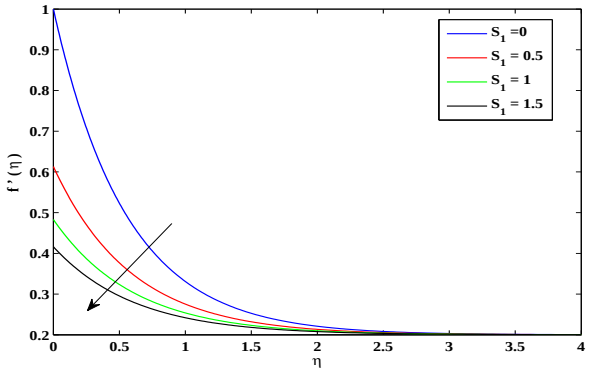

Fig. 10: Velocity profile for various values of velocity slip parameter S_1

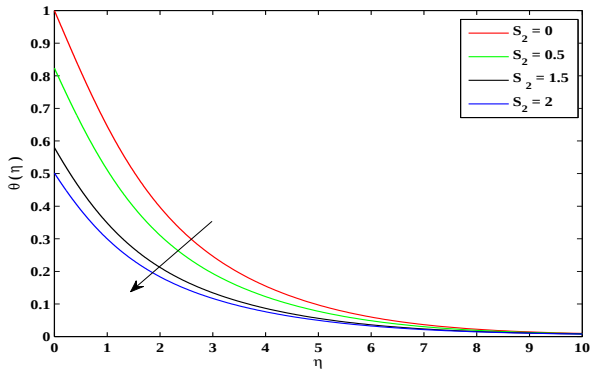

Fig. 11: Temperature profile for various values of thermal slip parameter S_2

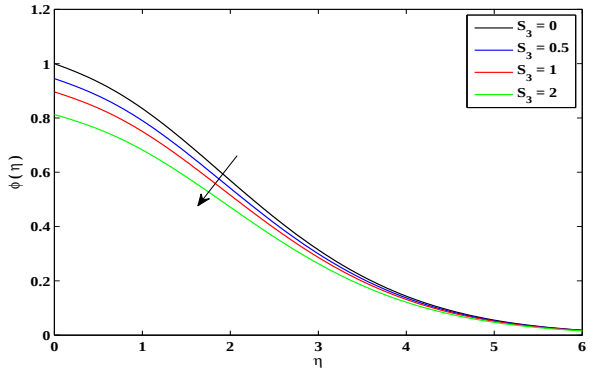

Fig. 12: Concentration profile for various values of solutal slip parameter S_3

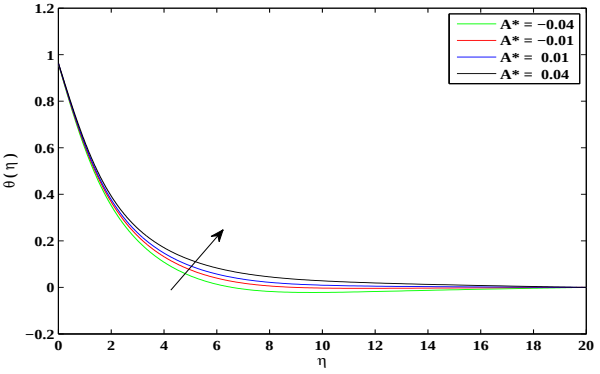

Fig. 13: Temperature profile for various values of A^*

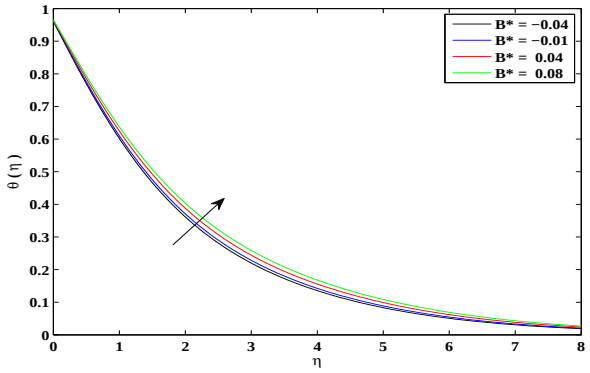

Fig. 14: Temperature profile for various values of B^*

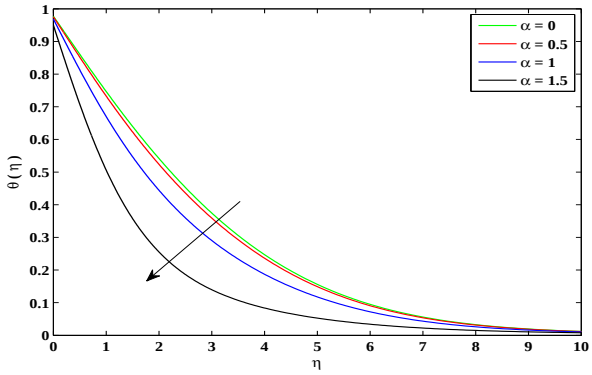

Fig. 15: Effect of α over temperature profile

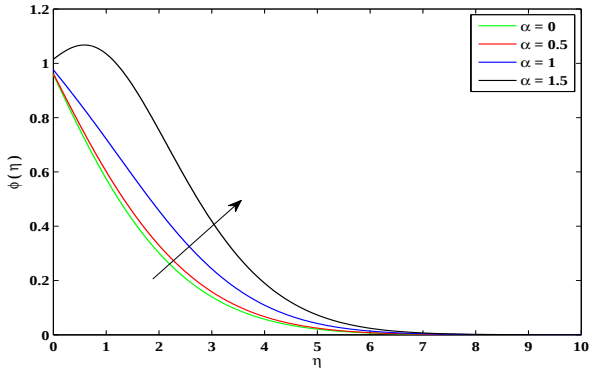

Fig. 16: Effect of α over concentration profile

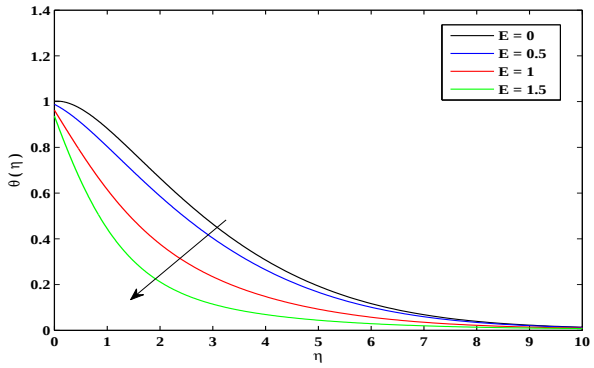

Fig. 17: Effect of E over temperature profile

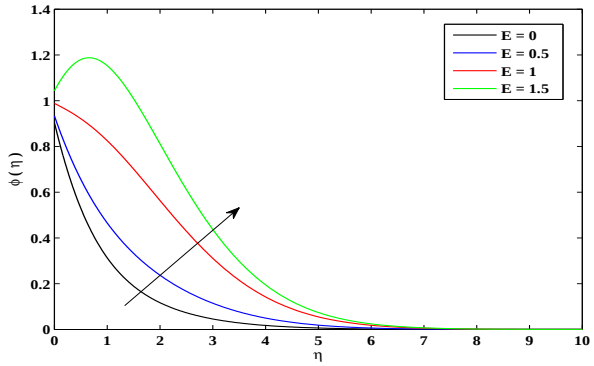

Fig. 18: Effect of E over concentration profile

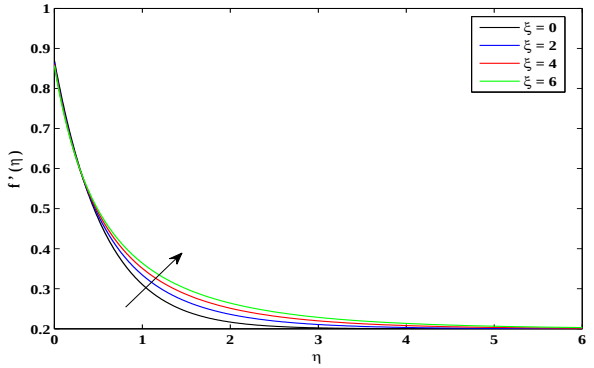

Fig. 19: Effect of ξ over temperature profile

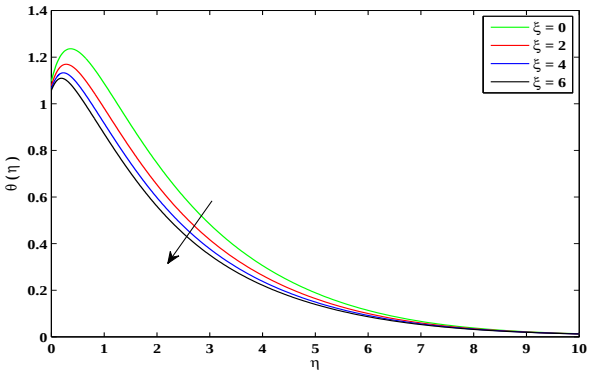

Fig. 20: Effect of ξ over concentration profile

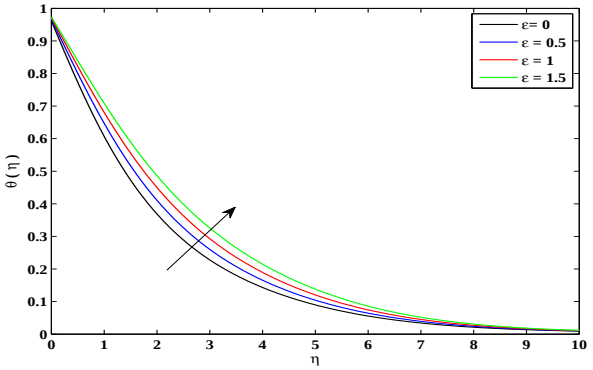

Fig. 21: Effect of ϵ over temperature profile

NOMENCLATURE

x	distance along the sheet
y	distance perpendicular to the sheet
u	velocity component in x - direction
v	velocity component in y - direction
β	Non Newtonian / Casson parameter
ρ	fluid density (assumed constant)
$\kappa(T)$	Temperature Dependent thermal conductivity
$\mu(T)$	Temperature Dependent fluid viscosity
U_w	stretching velocity of the sheet

U_∞	free stream velocity
T	Temperature
T_w	Wall Temperature
T_∞	Temperature at infinity
C	Concentration
C_w	Wall Concentration
D	Coefficient of mass diffusivity
B	Strength of magnetic field
σ	Electric conductivity
C_p	Specific heat at constant pressure
E_a	Activation energy
E	The non dimensional activation energy
ν	kinematics viscosity
μ_B	plastic dynamic viscosity of the Non-Newtonian fluid
p_y	yield stress of the fluid
ξ	Temperature Dependent viscosity parameter
ϵ	Temperature Dependent conductivity parameter
σ^*	Stefan Boltzmann constant
k^*	Absorption coefficient
Pr	Prandtl number
M	Magnetic parameter
R	Radiation parameter
Sc	Schmidt number
λ	velocity ratio parameter
α^2	dimensionless chemical reaction rate constant
Ec	Eckert number
η	similarity variable
$\theta(\eta)$	Non-dimensionless temperature function
$\phi(\eta)$	Non-dimensionless concentration function
$f(\eta)$	Dimensionless stream function

REFERENCES

[1] Hiemenz, K., *Die Grenzschicht an einem in den gleichfrmigen Flssigkeitsstrom eingetauchten geraden Kreiszylinder* , Dinglers Polytech Journal **326** 321–410, 1911.

[2] Homann, F., *Der Einfluss grosset Zhigkeit bei der Strmung um den Zylinder and um die Kugel*, Z. Angew. Math. Mech **16** 153–164, 1936.

[3] Pai, S.I., *Viscous Flow Theory I: Laminar Flow*, D.Van Nostrand Co., New York, 1956

[4] Schlichting, H., *Boundary Layer Theory* , McGraw-Hill Book Co., New York, 1968.

[5] Bansal, J.L. *Viscous fluid dynamics*, Oxford and IBH Pub. Co., New Delhi, 1977

[6] Chiam TC., *Stagnation-point flow towards a stretching plate*, J Phys Soc Jpn **63** 2443-4, 1994

[7] T.R. Mahapatra, A.G. Gupta, *Heat transfer in stagnation point flow towards a stretching sheet*, Heat Mass Transfer **38** 517-521, 2002

[8] C.Y. Wang, *Stagnation point flow towards a shrinking sheet* , Int. J. Non-Linear Mech. **43** 377-382, 2008.

[9] Y.Y. Lok, N. Amin, I. Pop, *Non-Orthogonal stagnation point flow towards a stretching sheet*, Int. J. Non-Linear Mech. **41** 622-627, 2006.

[10] Nazar R, Amin N, Filip D, Pop I., *Stagnation point flow of a micropolar fluid towards a stretching sheet*, Int J Non-Linear Mec **39** 1227-35, 2004.

[11] Layek GC, Mukhopadhyay S, Samad SKA., *Heat and mass transfer analysis for boundary layer stagnation-point flow towards a heated porous stretching sheet with heat absorption/generation and suction/blowing*, Int Commun Heat Mass Transfer **34** 347-56, 2007.

[12] K. Vajravelu, *Viscous flow over a nonlinearly stretching sheet*, Appl. Math. Comput. **124** 281-288, 2001.

[13] R. Cortell, *Viscous flow and heat transfer over a nonlinear stretching sheet*, Appl. Math. Comput. **184** 864-873, 2007.

[14] K.V. Prasad, K. Vajravelu, P.S. Dattri, *Mixed convection heat transfer over a non-linear stretching surface with variable fluid properties*, Int. J. Non-linear Mech. **45** 320-330, 2010.

[15] Hayat T, Javed T, Abbas Z., *MHD flow of a micropolar fluid near a stagnation-point towards a non-linear stretching surface*, Nonlinear Anal Real World Appl **10** 1514-26, 2009.

[16] A. Raptis, C. Perdikis, *Viscous flow over a non-linearly stretching sheet in the presence of a chemical reaction and magnetic field* , International Journal of Non-Linear Mechanics **41** 527-529, 2006.

[17] R. Bhargava, S. Sharma, H. S. Takhar, O. A. Bg, P. Bhargava, *Solutions for micropolar transport phenomena over a nonlinear stretching sheet* , Nonlinear Analysis: Modelling and Control **12** 45-63, 2007.

[18] W. P. Walawender, T. Y. Chen, and D. F. Cala, *An approximate casson fluid model for tube flow of blood*, Biorheology **12**(2) 111-124, 1975.

[19] M. Mustafa, T. Hayat, I. Pop, and A. Aziz, *Unsteady boundarylayer flow of a Casson fluid due to an impulsively started moving flat plate*, Heat Transfer **40**(6) 563-576, 2011.

[20] Rao AS, Prasad VR, Reddy NB, Beg OA, *Heat transfer in a Casson rheological fluid from a semi-infinite vertical plate with partial slip*, Heat Transfer-Asian Research 1-20, 2013.

[21] Qasim M, Noreen S, *Heat transfer in the boundary layer flow of a Casson fluid over a permeable shrinking sheet with viscous dissipation*, The European Physical Journal Plus **129** 1-8, 2014.

[22] Mukhopadhyay S, Mandal I.S. , *Boundary layer flow and heat transfer of a Casson fluid past a symmetric porous wedge with surface heat flux*, Chinese Physics B **23**, 044702-6, 2014.

[23] Venkatesan J, Sankar DS, Hemalatha K, Yatim Y, *Mathematical analysis of Casson fluid model for blood rheology in stenosed narrow arteries*, Journal of Applied Mathematics 1-11, 2013.

[24] Malik MY, Naseer M, Nadeem S, Rehman, *The boundary layer flow of Casson nanofluid over a vertical exponentially stretching cylinder*, Applied Nanoscience, 2013.

[25] Mukhopadhyay S, Bhattacharyya K, Hayat T, *Exact solutions for the flow of Casson fluid over a stretching surface with transpiration and heat transfer effects*, Chinese Physics B **22** 114701-6, 2013.

[26] Shehzad SA, Hayat T, Qasim M, Asghar S, *Effects of mass transfer on MHD flow of Casson fluid with chemical reaction and suction*, Brazilian Journal of Chemical Engineering **30** 187-195, 2013.

[27] K. Bhattacharyya, S. Mukhopadhyay, and G. C. Layek, *Slip effects on boundary layer stagnation-point flow and heat transfer towards a shrinking sheet* , International Journal of Heat and Mass Transfer **54** 308-313, 2011.

[28] K. Bhattacharyya, S. Mukhopadhyay, and G. C. Layek, *MHD boundary layer slip flow and heat transfer over a flat plate*, Chinese Physics Letters **28**(2), 2011.

[29] T. Fang, J. Zhang, and S. Yao, *Slip MHD viscous flow over a stretching sheetan exact solution* Communications in Nonlinear Science and Numerical Simulation **14**(11) 3731-3737, 2009.

[30] C.Y. Wang, *Flow due to a stretching boundary with partial slip an exact solution of the NavierStokes equations*, Chem. Eng.Sci. **57** 3745-3747, 2002.

[31] H.I. Andersson, *Slip flow past a stretching surface*, Acta Mech. **158** 121-125, 2002.

[32] P.D. Ariel, T. Hayat, S. Asghar, *The flow of an elastico-viscous fluid past a stretching sheet with partial slip*, Acta Mech. **187** 29-35, 2006.

[33] P.D. Ariel, *Two dimensional stagnation point flow of an elastico-viscous fluid with partial slip*, Z. Angew. Math. Mech. **88** 320-324, 2008.

[34] Z. Abbas, Y. Wang, T. Hayat, M. Oberlack, *Slip effects and heat transfer analysis in a viscous fluid over an oscillatory stretching surface*, Int. J. Numer.Methods Fluids **59** 443-458, 2009.

[35] Hayat T, Qasim M, Mesloub S, *MHD flow and heat transfer over permeable stretching sheet with slip conditions* , Int J Numer Meth Fluid **66** 963-75, 2011.

[36] M. Tencer, J. S. Moss, and T. Zapach, *Arrhenius average temperature: the effective temperature for non-fatigue wear out and long term reliability in variable thermal conditions and climates*, IEEE Transactions on Components and Packaging Technologies **27**(3) 602-607 2004.

[37] A.R.Bestman, *Radiative heat transfer to flow of a combustible mixture in a vertical pipe*, International Journal of Energy Research **15**(3) 179-184, 1991.

[38] M. A. Alabraba, A. R. Bestman, and A. Ogulu, *Laminar convection in binary mixture of hydromagnetic flow with radiative heat transfer*, Astrophysics and Space Science **195**(2) 431-439, 1992.

[39] R. Kandasamy, K. Periasamy, and K. K. S. Prabhu, *Effects of chemical reaction, heat and mass transfer along a wedge with heat source and concentration in the presence of suction or injection*, International Journal of Heat and Mass Transfer **48**(7) 1388-1394, 2005.

[40] O. D.Makinde, P. O. Olanrewaju, and W.M. Charles, *Unsteady convection with chemical reaction and radiative heat transfer past a flat porous plate moving through a binary mixture*

[41] O. D.Makinde and P. O. Olanrewaju, *Unsteady mixed convection with Soret and Dufour effects past a porous plate moving through a binary mixture of chemically reacting fluid*, Chemical Engineering Communications **198**(7) 920-938, 2011.

[42] Kh. Abdul Maleque, *Unsteady natural convection boundary layer flow with mass transfer and a binary chemical reaction*, British Journal of Applied Science and Technology (Science domain International) **3**(1) 131-149, 2013.

[43] Kh. Abdul Maleque, *Unsteady natural convection boundary layer heat and mass transfer flow with exothermic chemical reactions* , Journal of Pure and Applied Mathematics (Advances and Applications) **9**(1) 17-41, 2013.

[44] M.S. Abel, N. Mahesha, *Heat transfer in MHD fluid flow over a stretching sheet with variable thermal conductivity, non-uniform heat source and radiation*, Appl. Math. Model. **32** 1965-1983, 2008.

[45] Animasaun I.L, *Effects of thermophoresis, variable viscosity and thermal conductivity on free convective heat and mass transfer of non-darcian MHD dissipative Casson fluid flow with suction and nth order of chemical reaction*, J Nigerian Math Soc 2014;

[46] Makinde OD, *Effect of variable viscosity on thermal boundary Layer over a permeable flat plate with radiation and Convective surface boundary condition*, J Mech Sci Technol **26**(5), 2012.

[47] Salem AM, Fathy Rania, *Effects of variable properties on MHD heat and mass transfer flow near a stagnation point towards a stretching sheet in a Porous medium with thermal radiation*, Chin Phys B **21**(5), 2012.

[48] Prasad KV, Vajravelu K, Datti PS, *The effects of variable fluid properties on the hydromagnetic flow and heat transfer over a non-linearly stretching sheet*, Int J Ther Sci B **49** 603-10, 2010.

[49] Batchelor GK, *An Introduction to Fluid Dynamics*, London Cambridge University Press, 1987

DEPARTMENT OF MATHEMATICS, OSMANIA UNIVERSITY, HYDERABAD, TELANGANA.
E-mail address: monica.medikare@gmail.com
DEPARTMENT OF MATHEMATICS, OSMANIA UNIVERSITY, HYDERABAD, TELANGANA.
E-mail addresses: sucharithajoga@gmail.com
DEPARTMENT OF MATHEMATICS, NIZAM COLLEGE, OSMANIA UNIVERSITY, HYDERABAD, TELANGANA.
E-mail addresses: kishoresai09@gmail.com